ELSEVIER

Chemical Engineering Journal 76 (2000) 49–60

Chemical Engineering Journal

www.elsevier.com/locate/cej

Design, numerical simulation and experimental testing of a modified probe for measuring temperatures and humidities in two-phase flow

F. Kock, T.K. Kockel, P.A. Tuckwell, T.A.G. Langrish *

Department of Chemical Engineering, University of Sydney, Sydney 2006, NSW, Australia

Received 4 January 1999; received in revised form 20 July 1999; accepted 12 August 1999

Abstract

This paper describes the design of a modified gas sampling probe for measuring gas temperatures and humidities in a two-phase flow, based on the layout of Kieviet et al., [F.G. Kieviet, J. Van Raaij, P.J.A.M. Kerkhof, A device for measuring temperature and humidity in a spray drying chamber, Trans. Inst. Chem. Engrs, Part A, 75 (1997) 329–333]. This device separates small particles from the gas flow by means of the difference in inertia between the fluid and the particles. Two mechanisms of separation are employed successively, namely a swirling motion and a sharp change in direction of the flow. A small fraction of the clean flow is then directed to a thermocouple and subsequently to a dew-point hygrometer. The commercial computational fluid dynamics (CFD) package CFX4.2 has been used to assess the performance of the probe and to optimise the flow rates of the main and the clean air flow. Experimental testing confirms the prediction that this probe is able to measure temperatures and humidities in two-phase flows accurately down to particle diameters of 5 μm in droplet-laden flows. Due to deposition of wet solids on the swirl vanes, the separation performance for them decreases, so that only wet particles of more than 16 μm can be separated. ©2000 Elsevier Science S.A. All rights reserved.

Keywords: Modified probe; Swirling motion; Hygrometer; Fluid dynamics; Gas sampling

1. Introduction

In many industrial processes, two-phase flow involving sprays is utilised for mass or heat transfer processes, since the interfacial area is large, the turbulence levels are substantial and the transfer coefficients are high. Examples include spray dryers and wet flue gas scrubbers. Spray dryers may be up to 30 m high, and operational problems, such as the deposition of particles on walls, make it necessary to study the flow patterns using computational fluid dynamics (CFD) simulations. These simulations need to be validated with measurements, preferably on a full-scale plant. Temperature and humidity measurements inside these types of equipment are candidates for such validations.

However, measuring the air temperature and humidity in two-phase flow is complicated by the presence of particles. These particles will deposit on any probe or thermocouple placed directly in the chamber. In the case of liquid droplets, the temperature will approach the wet-bulb temperature, thus giving a false value. If the particles are solid or semi-solid, they will build up as a crust on a thermocouple, thus insulating it from the gas.

The same problem is associated with humidity measurement. Particles in an air stream will cause inaccurate measurements, and even cause damage to devices such as dew-point hygrometers. A wet bulb will also become encrusted with solids during evaporation, and hence give false readings.

Here, modifications are presented to a device originally developed by Kieviet et al. [6], which is suitable for preventing these particle depositions. CFD calculations have been performed to estimate the performance of the device and to predict under which boundary conditions the device might fail. Thorough testing of the device has confirmed these simulations and also shows that effects which were not taken into account by the simulation, such as formation and creeping of a liquid film and clogging of the vanes by solid depositions, do not jeopardise the use of the device too greatly for practical use.

First, previous devices for performing these measurements are discussed.

2. Literature review

Several ways to measure the temperature and humidity distribution in a spray-drying chamber are mentioned in the literature.

* Corresponding author. Tel.: +61-02-9351-4568; fax: +61-02-9351-2854.

1385-8947/00/$ – see front matter ©2000 Elsevier Science S.A. All rights reserved.
PII: S1385-8947(99)00113-8

Physical film removal. One simple solution is to make the measurements with an unprotected probe until the probe is covered with liquid. Then the probe can be taken out for cleaning, and another set of measurements can be started until the probe is covered again. This is feasible in flows with low-density droplet sprays, but it is unsuitable for most industrial applications [6].

Another disadvantage is that the cycle time for measurements is limited and difficult to estimate, as particles could be expected to immediately affect measurements in a dense spray. Furthermore, frequent removal of the thermocouple from a spray dryer for cleaning is time consuming and tedious, resulting in infrequent, inaccurate measurements.

Shielding from particles. Another approach is to prevent particles from depositing on the probe. A simple, one-sided shield has been presented by Papadakis [10]. The drawback of this solution is that it only prevents particle deposition from mainly one direction and is therefore not applicable for measurements in swirling flow domains.

An extended shield, which surrounded the thermocouple, has been presented by Goldberg [4]. This leads to the problem that the probe is measuring the temperature of stagnant air, which is surrounded by cooler air adjacent to the walls of the shield.

A solution to this drawback has been described by Nijhawan et al. [9]. The device containing a thermocouple is aspirated and still surrounded by a shield to prevent deposition of particles, but the device is quite bulky and has several sleeves and tubes which are difficult to build.

Particle removal by filters or tangential cyclones. One approach to developing a temperature and humidity measuring device relies on protecting the thermocouple from being hit by particles by removing the particles from the gas stream. The clean gas stream can then be fed to a hygrometer (located outside the spray dryer) for humidity measurement.

This separation could be achieved through a filter arrangement. However, in a system containing sticky particles and liquid the filters would clog up rapidly and require regular replacement or cleaning. As air is passed through the wet filter, evaporation would occur and the air stream would be cooled, resulting in a measured temperature less than the real temperature and a measured humidity larger than the real humidity. Thus, filtering to clean the air stream is not a convenient or accurate way to measure the air temperature.

Another commonly used method for separating gas and solid streams is to utilise the difference in inertia of the two phases. Traditionally, this has been achieved by using a tangential (reverse-flow) cyclone. However, its relative bulk and size of at least 10 cm prevents the cyclone from being inserted into a vessel. This cannot be overcome by removing a sample of the two-phase mixture, followed by separation in a cyclone outside the dryer, because heat losses in the connecting pipe work would result in a temperature reduction in the gas.

Table 1
Separation quality in percent for various outer tube velocities, as numerically predicted by Kieviet et al. [6] (the inner tube velocity was kept constant at 4 m/s)

Outer tube velocity (m/s)	Particle diameter (μm)				
	1	2	4	8	16
5	28	31	46	67	100
7	45	48	56	85	100
9	49	52	68	96	100
11	45	56	77	100	100

Table 2
Separation quality in percent for various inner tube velocities, as numerically predicted by Kieviet et al. [6] (the outer tube velocity was kept constant at 9 m/s)

Outer tube velocity (m/s)	Particle diameter (μm)			
	1	2	4	8
2	77	77	88	100
3	54	67	75	100
4	52	55	72	96
8	33	–	–	–

The Kieviet "micro-separator" temperature and humidity measurement probe. Kieviet et al. [6] have presented a different approach to prevent particle deposition on the measuring devices. Their device removes particles from the fluid before it encounters the temperature and humidity measuring equipment. Rather than using a cyclone, which is readily blocked by sticky particles and has a large volume considering the small amount of air that needs to be measured, a sharp change in direction of the gas flow is used to separate it from the particles. A flow reversal is achieved by using two coaxial tubes, the inner pipe being closed at the side facing the chamber. Part of the flow is sucked into the inner tube, the flow having to make a complete change in direction. Due to their inertia, many of the particles cannot follow the reversed stream and therefore do not enter the inner tube. Here, the thermocouple is located, yielding the temperature of the clean gas, and the gas is then pumped to a dew-point hygrometer. This concept of removing particles from the gas stream is called a *micro-separator*.

Several CFD simulations were carried out by Kieviet to test the micro-separator. These included varying the outer tube velocity, varying the inner tube velocity, and changing the geometry of the inner pipe. As expected, the separation quality increased as the outer tube velocity increased, since the particles had a greater momentum and were less likely to undergo a change in direction. Similarly, as the particle size increased, the separation efficiency increased (Table 1). With increasing inner tube velocity, the separation efficiency decreased (Table 2). It was found that none of the geometry alterations increased the separation efficiency when compared with the plain inner tube (Table 3).

This device was operated at an inner flow of 1.5 m/s, which was measured with a rotameter. This value was chosen

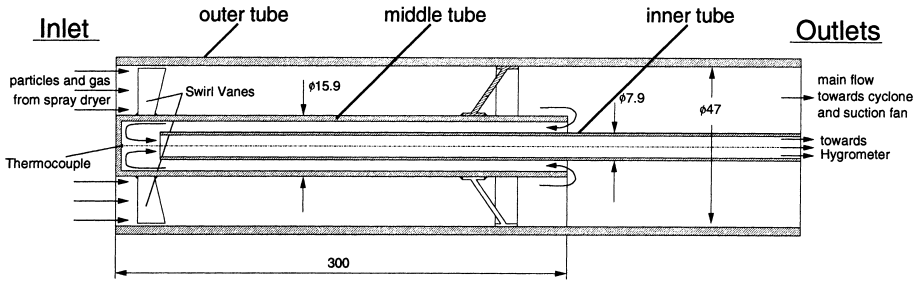

Fig. 1. Geometry of the microseparator.

Table 3
Separation quality in percent of various inner tube geometries, as numerically predicted by Kieviet et al. [6]

	Particle diameter (μm)				
	1	2	4	8	16
Open tube	75	75	88	99	100
Holes	78	82	80	85	92
Sharp tip	70	75	74	92	100

on the basis of the pressure drop in the inner tube. The outer flow rate was set to 9 m/s, also using a rotameter. A small tangential cyclone on the outer tube prevented clogging of the rotameter and blower.

To test the effectiveness of the microseparator, it was held under a spray consisting of 31 μm maltodextrin particles. For 2 h, the microseparator was positioned horizontally, 50 cm beneath the vertically positioned nozzle. The microseparator was then disassembled and the inner pipe was inspected for signs of maltodextrin. None was found in the inner tube, on the thermocouple or in the inner rotameter, and thus the microseparator was found to function well.

Kieviet has also used the microseparator to measure the temperatures and humidities in a large pilot-scale spray dryer (Kieviet and Kerkhof [7]). The only problem encountered was that, while measuring spray close to the hot air inlet (195°C), a dry crust of maltodextrin several centimetres thick built up on the outer tube. This limited the measuring period at this location to several minutes.

After having reviewed former solutions and having discussed their advantages and drawbacks, the modified device will be presented.

3. Description of the modified device

The measuring device presented in this paper is based on the principle described by Kieviet et al. [6]. Particle sizes in commercial spray-drying chambers are expected to be in the range from 5 to 250 μm. Hence only the larger particles may be separated from the gas stream by means of a sharp change of direction in flow.

Basic concept and description of the altered design. In order to remove these particles from the gas stream, an additional concept is used in the probe described here. This principle is based on setting up swirl by curved vanes in the air inlet, thus removing further particles from the gas stream by means of depositing them on the walls of the tube. Following this axial cyclone, the flow reversal is then used as a second cleaning step, sucking the air out of a relatively particle-free inner flow zone.

A second improvement refers to the handling of the probe; the original device had the flow-reversal tube protruding from the main suction tube at right angles, and the sampling air stream was then externally pumped to a dew-point meter. This makes the apparatus difficult to insert into a small-diameter porthole. Here, a second central tube, concentric to the first inner tube and thus yielding a second flow reversal, gives a more compact design and is also simpler to build.

The probe consists of three coaxial tubes which form the microseparator (Fig. 1). The air is sucked into the outer tube of the probe with a fan at the outlet end. The sample air stream passes along the middle tube, which is closed at the side facing the measurement domain. Swirl vanes at the inlet of this annular cross-section set up a vortex, which forces sucked-in particles towards the wall. The swirl vanes are twisted so that they set up a potential vortex-type motion with a high tangential velocity at the inner diameter of the inlet, and this velocity gets smaller with increasing distance from the symmetry axis. The potential swirl gives the particles which are close to the wall of the middle tube a higher impulse to accelerate them towards the outer wall than particles which enter close to the outer wall.

The middle tube ends 300 mm downstream of the inlet, and a portion of the air is sucked into the annulus between the middle and the inner tube. Since the flow changes its direction, particles that are still in the stream cannot flow into the middle tube, and the thermometer is located at the end of this tube. After the second flow reversal, the inner tube with an inner diameter of 5 mm then leads the flow through a hose to the dew-point hygrometer.

After this overview of the modified probe, some features will be described more explicitly:

Material selection. Stainless steel was the most suitable option for the probe material. Since this specific probe was built to be utilised in a milk dryer, special hygiene standards are required, which can be met by stainless steel because of

its corrosion resistance and smooth, shiny surface ensuring easy cleaning and sterilisation.

Design of swirl vanes. The swirl vanes have been added to the probe to impart a tangential component to the flow. It has been observed that free swirls form a Rankine swirl flow pattern [5], which consists of a potential flow with a central rigid body swirl.

The transition radius r_{tr} between these two zones is a known function of the vortex strength. In this instance, it is chosen so that is equals the radius of the middle tube. Apart from the boundary layers directly at the walls, the flow in the annulus should then form a potential flow pattern. From this, a transition radius ratio of $(r/r_{max})_{tr} = 0.338$ follows, yielding a vortex strength of $\Gamma = 0.868\,m^2/s$.

With an axial velocity of 10 m/s, a tangential velocity is estimated to be 6.0 m/s at the outer radius of the vane; at the inner radius of 8.55 mm, the tangential velocity is 16.2 m/s.

Since the axial velocity is the same in both cases, the deflection of the flow by the vanes has to decrease with increasing radius; they have to be skewed. The angle of deflection increases from 28° at the inside to 52° at the outer wall. To reduce pressure drop and to simplify manufacture, the form of the vanes was chosen to be arcs of a circle, the whole vane being a part of a conical surface.

In order to prevent possible liquid films on the vane from being dragged to the central axis by the pressure difference in the swirl, the vanes are tapered towards the outer wall of the outer tube.

Swirl vane attachment and tube support. The vanes are welded to the middle tube, supporting it in the first part of the outer tube; a second support with inclined arms is welded to the end of the middle tube and then fixed at the outer tube with a screw.

Positioning of thermocouple. The thermocouple, a shielded K-Type with glass fibre insulation, is inserted through a hole in the nose of the middle tube and insulated against it with Teflon tape.

Air cleaning method for outer flow. A tangential cyclone connected to the end of the outer tube outside the vessel was the obvious method for removing the dust and droplets. This has the advantage that a sample of the powder can be collected at the bottom of the cyclone.

Suction fan selection. As an air pump for providing the flow rates for the outer and the inner tube, a common vacuum cleaner was used, and this was found to be the best solution for laboratory applications. It is designed to handle moderate to large amounts of dust in the suction air flow, and during the experiments, no operational problems occurred.

Outer and middle tube velocity and flow rate measurements. The pressure drop over the outer tangential cyclone was then calibrated with an orifice to yield the outer volumetric flow rate. This is a convenient method since no additional pieces of equipment such as rotameters have to be used, which would further increase the pressure drop. The accuracy of this device is governed by the accuracy of the pressure difference measurement, given that no clogging occurs in the cyclone. With the U-tube water manometer used here, a relative accuracy of ±5% for the flow rate was estimated.

The inner volume flow rate is determined by the pressure drop over a long thin tube. At the maximum flow rate through this tube, the flow stays in the laminar region, so the friction factor (f) is independent of the wall roughness and the equation $f = 64/Re$ can be utilised. The pressure drop was also monitored with a water-filled U-bend manometer, and the accuracy here was estimated to be ±10% because of the smaller pressure drop.

4. Numerical simulation

When operating the microseparator, the amount of particles which deposit on the walls of the tubes is dependent both on the absolute values and the ratio of the velocities in the outer and middle tube. A high velocity in the outer tube is needed to prevent particles from getting sucked into the middle tube, because the high impulse of the particles keeps them from turning into the middle tube.

In order to investigate which velocities are best for preventing most of the particles from getting sucked into the middle tube and thus depositing on the thermometer (causing the probe to fail), a CFD simulation of the flow pattern in the microseparator has been performed. The description of this simulation, including the model and grid, the results and a concluding discussion follow.

4.1. Numerical method

To solve the problem of a swirling tube flow simulation numerically, the computational space has been divided into discrete elements. The time-averaged Navier–Stokes equations have been solved, together with a turbulence model to address the closure problem as described in [2].

A commonly used turbulence model is the k–ε model, which introduces two additional equations for the turbulence kinetic energy k and the dissipation rate ε, [8]. Since this model assumes the turbulence to be isotropic, it is not appropriate for simulating a swirling tube flow, where the turbulence phenomena are expected to be highly anisotropic. Investigations have shown that the more complex differential stress model (DSM) takes this anisotropy into account [12] without causing excessive computational effort.

In order to obtain mass conservation in the non-linear conservation equations for incompressible flows, so called velocity–pressure coupling algorithms have been introduced. The algorithm used in these sets of simulations is the SIMPLEC method. The improved Rhie–Chow algorithm has been used to obtain a solution on a grid with variables which are all located at the same positions [11].

Various discretisation methods are available. Following the recommendations of Shore et al. [12], the differencing scheme used in this set of simulations (orthogonal

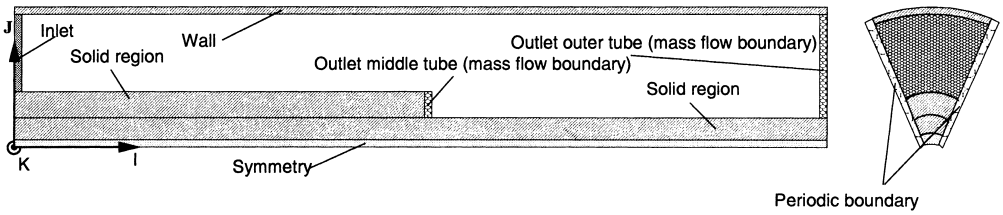

Fig. 2. Boundary conditions for the simulation.

grid) is the UPWIND scheme for the velocities, the central differencing scheme for pressure and the HYBRID scheme for all other variables [1]. The algebraic multigrid (AMG) solver has been used for the inner iteration for all variables.

The convergence criterion in this set of simulations is the relative error. A simulation is considered to be well converged if the mass source residuals have reached a value of 0.1% of the total mass flux through the flow domain, which was found to be sufficient for this type of problem by Fletcher et al. [2]. The solutions were under-relaxated, with under-relaxation factors between 0.1 and 0.2 for all variables except pressure, where an under-relaxation factor of 0.7 was used. The DSM model needs about 2500 iterations to achieve a converged solution.

Using converged solutions of these flow patterns, particle trajectories are calculated. These trajectories are calculated by integrating the equations of motion for each particle in the surrounding air flow, including the drag forces. These drag forces depend on the difference in velocity between the particles and the air-flow. After this step, the influence of the particle has to be taken into account for the next calculation of the flow field; seven of these iterations have been found to reach sufficient convergence such that the flow field does not change significantly from iteration to iteration. The particle mass flow rate in these calculations has been set to a value of 8×10^{-4} kg/s according to values obtained during measurements in an existing spray dryer. The calculation of particle trajectories is also given in [2]. Turbulent dispersion has been accounted for using an eddy interaction model [13].

4.2. Boundary conditions of the computational flow domain

The topology for the simulation of the microseparator outlined in the description of the modified device has been set up using the `CFX Build4` package. The flow pattern has been simulated using grids with both two-dimensional cylindrical coordinates and three-dimensional Cartesian coordinates. As the resulting flow patterns show no significant difference, all further investigations have been made using the two-dimensional model due to simplicity and lower computational effort.

Topology and grid. The computational space is bounded by six blocks using cylindrical coordinates. Patches are used to define the boundary conditions for the flow domain. A sketch of these patches is given in Fig. 2.

The inlet into the domain is set up by a simple Dirichlet boundary condition. As the flow domain of interest is only the outer tube, the flow patterns in the inner and middle tubes are not calculated. Simulating the flow in the middle and inner tube would be difficult, as the difference between the adjacent walls is far too small to make the use of the log law for the wall treatment valid. Multiple outlets are defined by the use of mass flow boundaries.

A symmetry boundary at the low J-face and periodic boundaries at the low and high K-faces have ensured that the flow domain is cylindrical and axially symmetric.

An orthogonal grid has been set up. It contains 60 elements in the axial flow direction with a logarithmic distribution, causing the grid to be finer at the region of interest, which is the outlet into the middle tube. To overcome convergence difficulties, the grid contains four elements in the angular direction. In the radial direction the grid is set up in such a way that the elements adjacent to the walls are thick enough to exclude the boundary layer, with values of y^+ near the wall of over 30. This value of y^+ ensures that the use of wall functions is valid in our flow domain. The resulting grid can be seen in Fig. 3. The choice of computational grid is constrained by the absolute need to have a specific range of y^+ values. Within this constraint, another grid (with 20% more node points) gives the same velocity profiles in radial direction within 4% at a point 35 cm downstream of the inlet, which is just behind the flow reversal.

Inlet boundary. In order to take the swirl vanes into account, a circumferential velocity profile is set at the inlet boundary of the flow domain. The free vortex flow distribution described in the section on the layout of the vanes has been implemented in the user Fortran routines of the `CFX4.2` package.

In order to optimise the separation effect of the probe, various axial velocities have been set up at the inlet, ranging from 6 to 12 m/s, which result in Reynolds numbers in the range from 16 450 to 32 900 based on the hydraulic diameter of the outer flow region.

Outlet boundaries. As the aim of these investigations is to get an insight into which velocities in the outer and middle tube are most suitable to keep particles from depositing on the thermocouple, boundary conditions have to be set up to define the ratio of the outflows from the outer tube to the

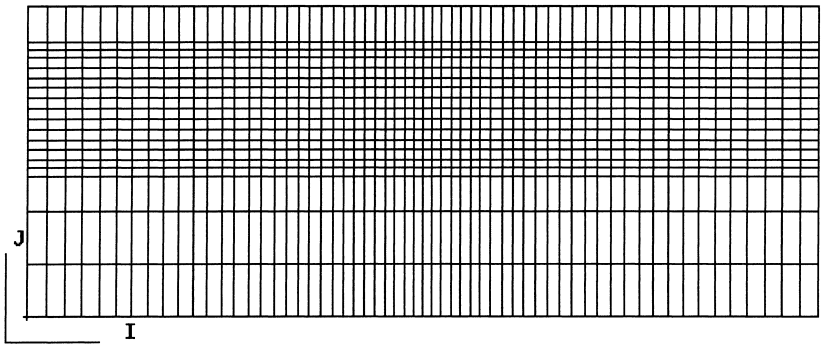

Fig. 3. Orthogonal grid, using 3240 elements, I/J-scale=10.

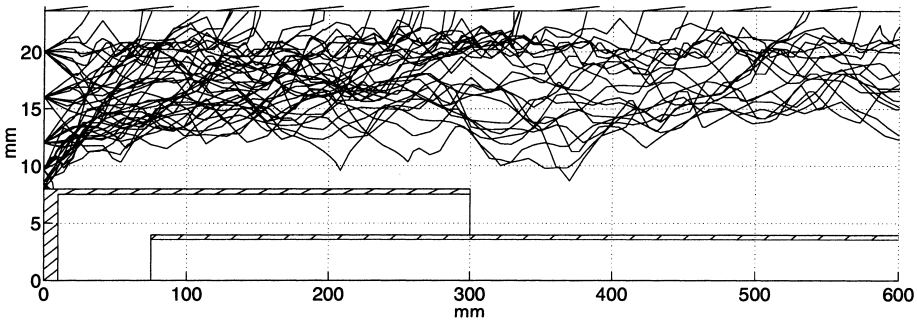

Fig. 4. Swirl included; particle size 5 μm; $v_{outer} = 6\,m/s$; $v_{middle} = 5\,m/s$.

outflow from the inner tube. By setting up the ratio of mass flux leaving through the outer and inner tube and knowing the velocity at the inlet, the velocity in the inner tube is fixed. Considering an incompressible flow, the mass flux into the flow domain is

$$\dot{m}_{o_{in}} = \varrho \cdot A_o \cdot v_{o_{ax}}, \tag{1}$$

where ρ is the fluid density, A_o is the cross-sectional area at the inlet of the outer tube and $v_{o_{ax}}$ is the axial velocity at the inlet of the outer tube. The mass flux through the outlet of the outer tube is

$$\dot{m}_{o_{out}} = \dot{m}_{o_{in}} - \dot{m}_{m_{out}}. \tag{2}$$

Therefore the ratio of the mass fluxes leaving the tubes becomes

$$\frac{\dot{m}_{o_{out}}}{\dot{m}_{m_{out}}} = \frac{\dot{m}_{o_{in}}}{\dot{m}_{m_{out}}} - 1 = \frac{A_o \cdot v_{o_{ax}}}{A_m \cdot v_{m_{ax}}} - 1, \tag{3}$$

where A_m is the cross-sectional area at the outlet of the middle tube and $v_{m_{ax}}$ the axial velocity at the outlet of the middle tube. The command language of CFX4.2 needs a fractional value for each flux when defining multiple outlets. Thus the fractional mass fluxes will be referred as M_o and M_m for the outlet of the outer tube and the outlet of the middle tube, respectively

$$M_o + M_m = 1. \tag{4}$$

Using Eq (3), the fractional mass fluxes become

$$M_o = 1 - \frac{A_m \cdot v_{m_{ax}}}{A_o \cdot v_{o_{ax}}}, \qquad M_m = 1 - M_o. \tag{5}$$

4.3. Results of the numerical analysis

In order to estimate the performance and the optimal set point of the flow rates, simulations have been performed with different sets of boundary conditions. The velocities in the outer tube have been varied from 6 to 12 m/s in 2 m/s steps, and in the inside tube from 2 to 5 m/s in 1 m/s steps, respectively. At each pair of velocities, one simulation has been made including the potential vortex, and one simulation has been made without consideration of this swirl, in order to show the effectiveness of the newly introduced swirl vanes.

Particle trajectories have been obtained with two particle sizes, 5 and 250 μm, to investigate if the probe is effective with both small and large particles. Particles have been started at an initial distance of 8.0, 8.5, 9.5, 12.0, 16.0 and 20.0 mm from the symmetry axis, having an initial velocity equal to that of the air. Ten particles have been injected from each starting point. A coefficient of restitution of zero was assumed, i.e., the calculation of the particle tracks stops if a particle hits a wall.

With the swirl vanes, particles have not been predicted to be sucked into the middle tube with any of the above described boundary conditions. This finding indicates the high effectiveness of the modified device for separating particles from the measurement air stream. The following sections demonstrate the improvement of the performance of a microseparator on sample particle trajectories. The following influences are investigated in detail: The influence of the swirl (Figs. 4 and 5), of the particle size (Figs. 4 and 6), of the velocity in the outer pipe (Figs. 4 and 7), of the ve-

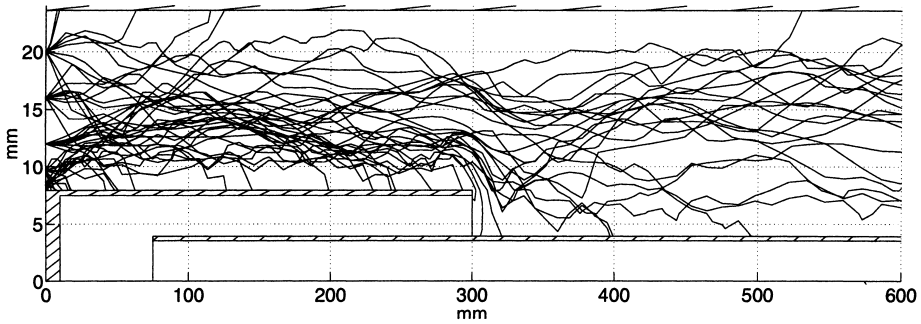

Fig. 5. No swirl; particle size 5μm; $v_{outer} = 6\,m/s$; $v_{middle} = 5\,m/s$.

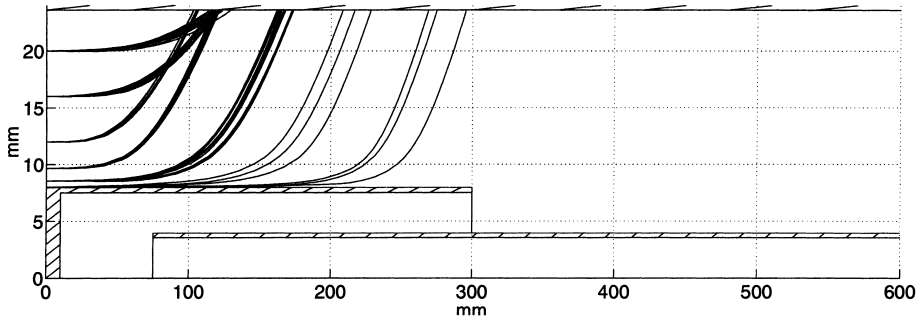

Fig. 6. Swirl included; particle size 250 μm; $v_{outer} = 6\,m/s$; $v_{middle} = 5\,m/s$.

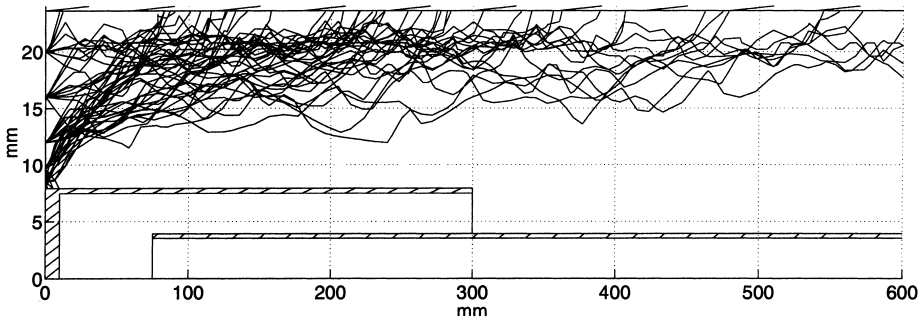

Fig. 7. Swirl included; particle size 5 μm; $v_{outer} = 12\,m/s$; $v_{middle} = 5\,m/s$.

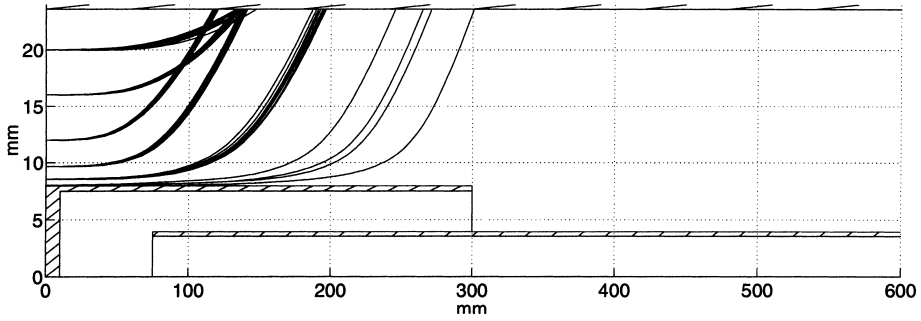

Fig. 8. Swirl included; particle size 250 μm; $v_{outer} = 12\,m/s$; $v_{middle} = 5\,m/s$.

locity in the middle pipe and of the initial particle position (Fig. 8).

Influence of the swirl. The superimposed vortex is predicted to be the most significant influence on the particle separation. Figs. 4 and 5, showing the particles trajectories of particles 5 μm in diameter, a velocity of 6 m/s in the outer tube, 5 m/s in the middle tube, with and without an superimposed swirl, demonstrate the high effectiveness of the swirl vanes for separating small particles from the air stream. The particles are clearly pushed to the outer region of the swirling

flow domain, and thus are kept far away from the inlet to the middle tube. Imposing no swirl allows particles to be sucked into the middle tube.

Influence of the particle size. Figs. 4 and 6 show particle trajectories of particles 5 and 250 μm in diameter, but otherwise having the same boundary conditions. The results demonstrate that both extrema of particle sizes, which are expected to occur in spray-drying chambers, are likely to be completely separated from the gas stream and prevented from flowing into the middle tube.

Influence of the velocity in the outer tube. Comparing Figs. 4 and 7 demonstrates that the velocity in the outer tube has only a slight impact on the particle trajectories. Smaller particles are seen to be pushed slightly further away from the inlet into the middle tube. However particles 250 μm in diameter tend to deposit in the same region on the outer wall, even when injected near the boundary layer of the wall at the middle tube. This result shows that the performance of the probe is predicted to be largely independent of the velocity in the outer tube.

Influence of the velocity in the middle tube. When setting up a swirl at the inlet to the probe, the particles are kept far away from the inlet to the middle tube, so that no influence of the velocity in the middle tube can be seen in either simulation.

Influence of the initial particle position. Figs. 6 and 8 demonstrate that large particles, when entering the flow domain sufficiently remote from the walls, deposit in the same region on the outer wall. This can be explained by the tangential velocity field, which has a higher tangential velocity at a position closer to the symmetry axis than at a position further away from the axis. This forces particles which enter the domain at a position closer to the symmetry axis to gain a higher circumferential impulse than particles starting at a larger distance from the symmetry axis, thus resulting in particles depositing on the same region of the outer wall. This explanation is not true for particles entering the domain close to the wall of the middle tube, which travel significantly further. This is because these particles enter the boundary layer and are not fully exposed to the tangential velocity field. These particles are forced into the bulk stream only by turbulent dispersion, before being exposed to the potential vortex.

5. Estimation of the temperature drop caused by evaporation of deposited particles

The results of the simulation show that all particles having typical sizes for spray-drying applications are accelerated toward the outer wall of the probe. In particular, larger particles, having sizes in the order of 250 μm, are likely to be deposited on the outer wall, as shown in Figs. 6 and 8. As the wet particles still contain a considerable amount of water, evaporation of this water film could lower the temperature of the air which is sucked into the middle tube, thus giving false temperature readings. This effect needs to be estimated.

Table 4
Values used for the estimation of the evaporation-related temperature drop

Inlet velocity	12 m/s
Re number[a]	32 900
Sc number	0.52
Sh number[b]	77.5
Mass transfer coefficient[a]	53.37×10^{-3} m/s
Max.conc. driving force (sat. conc. at 80°C)	15.61 mol/m^3
Mass flux of water vapour	0.66 g/s
Required heat flux for evaporation	1.66 W
Calculated temperature drop	0.075 K

[a]Based on the hydraulic diameter.
[b]Using the modified correlation by Pethukov and Kirilov [3].

The worst case has been evaluated, in which a complete film of water covers the outer wall of the tube from the inlet up to the inlet to the middle tube, i.e., a film of 300 mm length. Furthermore it is assumed that the concentration of water vapour on the wall equals the saturation concentration at the wet-bulb temperature and the concentration in the bulk flow is zero. Considering that in the worst case scenario of a constant water film on the outer wall (Table 4), evaporation leads to a temperature drop in the air of the order of 0.075 K, the influence of the evaporation of deposited particles on the measurement air flow can be neglected.

6. Probe testing and optimisation

6.1. Method of testing

After the above theoretical considerations, the probe was tested in a pilot-scale spray dryer to assess its usefulness when faced with sprays of liquid and of semi-dry particles. Apart from validating the simulations, the real behaviour of the particles can be observed, such as the formation and transport of liquid films or the clogging effects of sticky particles.

Fig. 9 shows that the particles present in the experimental dryer are much smaller than those produced by a full-scale dryer due to the use of a two-fluid nozzle in the experimental (model) dryer rather than the rotary atomiser in the full-scale dryer. In the model dryer, less than 5% of particles are larger than 50 μm, and the smallest particle size present is 1 μm. The modal size fraction consists of 22 μm particles. If the probe does not fail under laboratory conditions, it is unlikely to fail in the full-size dryer with larger particle sizes, in terms of particles interfering with temperature and humidity measurements.

There were several problems involved with physically testing the probe to get quantitative separation efficiency results:

- The end of the middle tube was welded closed, so seeing or inserting anything far into the middle tube was not feasible.

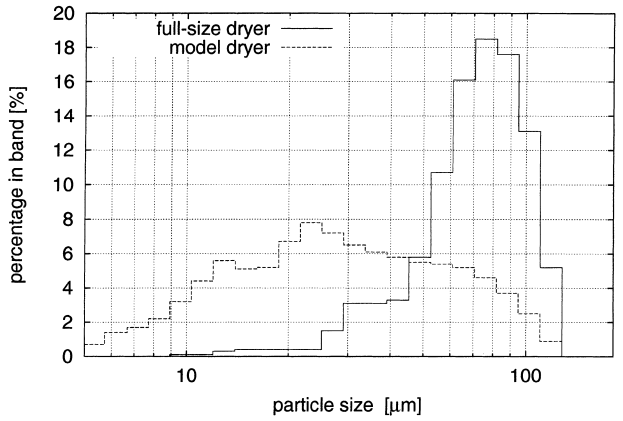

Fig. 9. Particle size distributions for a full-size and for the model spray dryer used in this investigation.

- The number of particles entering the middle tube was too small to measure them accurately by weighing or by conventional methods.
- The particles in the clean air stream could not be collected in order to measure the separation efficiency. If there were any particles in the air stream, the majority would adhere to the walls of the inner tube or silicon tubing.

Qualitative estimates of the separation performance could be obtained by visually inspecting the number of particles sticking to the middle tube wall at different flow rates. However, this is not an accurate or effective way of optimising the performance of the probe, and thus practical testing alone could not determine the most suitable middle and outer tube velocities.

The middle tube was then visually inspected for signs of droplets entering it, and thus the separation quality resulting from each velocity combination was evaluated. The separation efficiency of the different flow rates was compared by describing the amount of liquid that entered the middle tube. Any liquid droplet entering the middle tube and touching the walls evaporated very quickly, leaving an opaque film. The degree of film formation could be described, and although qualitative, this method of comparison gave an indication as to which velocity combinations successfully cleaned the air.

The thermocouple was also inspected to assess the separation quality. The presence of a film on the thermocouple indicates interference with temperature measurement, and the presence or absence of this film was also qualitatively described for each velocity combination.

The middle tube was also examined for evidence of liquid dribbling along the its outer wall and being sucked into the clean air inlet. It was expected that this could be distinguished from liquid droplets that contacted the tube wall and evaporated by long trails of liquid film, compared with spots of film.

Table 5
Results of the visual inspection of the probe for the tests with droplets[a]

v_{mid} (m/s)	Outer tube velocity, v_{out} (m/s)		
	6	8	12
1	(⊙/⊙)	(⊙/⊙)	(⊙/⊙)
3	(⊙/⊙)	(⊙/⊙)	(⊙/⊙)
5	(⊖/⊙)	(⊙/⊙)	(⊙/⊙)

[a]Entries as pairs (middle tube/thermocouple): (⊙) no visible deposition; (⊖) some deposition.

6.2. Tests with droplets

The tests have been carried out with skim milk concentrate and the air temperature in the drying chamber, which was the inlet temperature to the probe, was ≈ 80°C.

The probe was tested at a middle tube flow rate of 1, 3 and 5 m/s. At each of these middle tube flow rates, the outer tube was tested at 6, 8, and 12 m/s, giving a total of nine different combinations of flow rates.

After insertion into the dryer, air was sucked through the probe for a period of 5 min at the specified middle and outer tube velocities. The end of the probe (the entrance to the outer tube) was placed in the centre of the dryer, the region of greatest spray density. After the test, the probe was removed from the dryer and the middle and the inner tube (as well as the thermocouple) were removed for visual inspection. “Some deposition” was defined as less than 25% coverage after 15 min of operation and “heavy deposition” signifies more complete coverage. The results are given in Table 5.

At the lowest outer tube velocity obtainable by the flow control (6 m/s) and the highest middle tube velocity (5 m/s), a small amount of film was observed inside the middle tube. This imperfect separation performance was due to unfavourable conditions for the flow reversal mechanism. These findings are consistent with the predictions of the simulation, in that the probe is more likely to fail at low outer and high middle tube velocities.

As the probe was only observed to fail at this high middle tube velocity, it is recommended that the middle tube velocity be maintained at a low level (< 3 m/s) when taking measurements.

6.3. Test with powders

The probe was also tested in the same experimental spray dryer while milk powder was being produced. The inlet air temperature to the probe was ≈ 100°C. Again, the dryer was allowed to come to steady state for 1 h and the entrance of the probe was pushed to the centre of the dryer, into the middle of the spray cloud.

The method of testing was similar to that described for testing in the liquid region. Middle tube velocities of 1 and 5 m/s were tested, in combination with outer tube velocities of 6, 10 and 12 m/s. Again, a period of 5 min per test was used before the optical assessment of depositions.

Table 6
Results of the visual inspection of the probe for the tests with particles[a]

v_{mid} (m/s)	Outer tube velocity, v_{out} (m/s)		
	6	8	12
1	(⊕/⊙)	(⊖/⊙)	(⊖/⊙)
5	(⊕/⊖)	(⊖/⊖)	(⊖/⊙)

[a]Entries as pairs (middle tube/thermocouple): (⊙) no visible deposition; (⊖) some deposition; (⊕) heavy deposition.

The results are shown in Table 6 .

Table 6 shows that the probe is not as effective when trying to separate semi-dry powder particles and air. During the 5 min testing period, some powder entered the middle tube for all of the velocity combinations tested. The amount of powder in the middle tube increased as the outer tube velocity decreased and the middle tube velocity increased. Only at the maximum outer tube velocity (12 m/s) was there only a very small amount of powder in the inner tube, and thus adequate separation performance.

These results are different from those obtained from testing the probe with liquid droplets, which were of the same size and could be easily separated from the air stream. This difference can be explained by the large build up of milk particles on the swirl vanes. For every run, the sticky milk particles totally clogged up the swirl vanes and rendered them useless in creating a swirl. Without a swirl, the particles were not forced to the outer tube walls and many would have remained near the middle tube suction, enabling them to be sucked in. The swirl vanes did not clog when testing with liquid droplets, and so the swirl would have aided in the excellent separation performance achieved.

Due to the clogging of the swirl vanes, the flow reversal is the only mechanism being utilised for obtaining a clean air stream when obtaining an air/powder sample. In conjunction with the flow simulation, this explains why the largest outer tube velocity and the smallest middle tube velocity achieves the best separation performance. For this reason, it is recommended to operate the probe with an outer tube velocity of 12 m/s and the lowest practical middle tube velocity, in order to obtain the full benefit of the flow reversal.

6.4. Comparison between the probe and an unshielded thermocouple

In order to test the accuracy obtained by using the probe compared with an unshielded thermocouple, the readings of an unshielded thermocouple at the probe inlet have been recorded together with the probe thermocouple temperature while being exposed to a droplet spray of water in the model dryer.

The velocity of the air in the outer tube was set to 12 m/s, and the middle tube was tested at velocities of 1, 2, 3 and 5 m/s. For each middle tube velocity tested, the temperature of the air inside the dryer was increased gradually from ≈ 35–45°C.

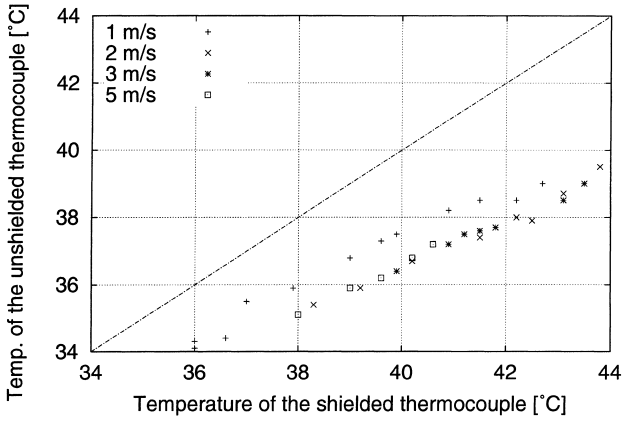

Fig. 10. Comparison between the temperature readings of an unshielded thermocouple and the shielded thermocouple; middle flow velocity has been varied.

Fig. 10 shows the temperature recorded for the unshielded thermocouple plotted against that recorded by the shielded thermocouple. The following observations were made:

- For all temperature measurements, the temperature of the air measured by the probe thermocouple was substantially larger than that measured by the thermocouple in contact with the spray. This difference ranges from 2 K for a probe temperature of 36°C, up to 4.5 K for a probe temperature of 44°C. The difference increases with increasing air temperature because the cooling effect of the evaporating film on the unshielded thermocouple becomes more apparent at higher temperatures, where the evaporation rate is highest.
- For middle tube velocities of 2, 3 and 5 m/s, there is virtually no effect of the air velocity on temperatures measured from the shielded thermocouple compared with the temperatures measured from the unshielded thermocouple. This indicates that, for these velocities, the shielded temperature measurement is accurate. At a middle tube velocity of 1 m/s, however, the shielded thermocouple measurement (compared with the unshielded thermocouple measurement) does not follow the same trend as the other middle tube velocities. For a given unshielded thermocouple temperature reading, the shielded thermocouple reading is ≈ 2 K less than the trend followed by the rest of the data. This indicates that heat is being transferred between the middle tube walls and the air stream, thus cooling the air stream before temperature measurement. As the middle tube air velocity and flow rate is increased, this heat transfer does not noticeably decrease the temperature of the air stream, and thus a temperature measurement can be accurately taken.

After comparing the temperature measurements obtained by using the probe against measurements obtained by an unshielded thermocouple, it is clear that more accurate temperature measurements can be obtained by using the probe, provided that the velocity in the middle tube does not fall below 2 m/s.

7. Discussion

In this paper, a modified design of a gas suction probe is described which is capable of measuring the temperature and humidity of gas in two-phase flows. Possible applications are measurements inside spray dryers or wet flue gas scrubbers.

Design. The design of this probe was based on a probe previously developed by Kieviet [6] with several modifications:

- A second separation stage is employed prior to the 180° flow reversal. It relies on a axial cyclone mechanism to force the particles or droplets to the outer region of the outer tube. The entrance of the middle tube, into which the measuring sample flow is sucked, is kept relatively particle-free. The swirl vanes at the inlet of the suction probe were designed to develop a potential swirl, with the middle tube radius defined as the critical radius of the swirl. By designing curved vanes which directly created a natural swirl at a certain axial velocity, the efficiency of the swirl in creating a clean air core after a certain length was maximised and the pressure loss minimised.
- A third tube has been included in the design, giving a second flow reversal in order to avoid a suction tube outside the main probe tube.
- The flow rate in the outer tube is assessed by measuring the pressure drop across the tangential cyclone at the end of the probe, while the inner flow rate is monitored by the pressure drop across a laminar flow tube.
- Supports for the inner and middle tubes were necessary for correct positioning. The shape of these was designed such that any liquid droplets contacting these supports would be forced to the outer tube wall and not interfere with temperature measurement by being sucked into the middle tube.

Computational analysis. The flow pattern inside the tube has been calculated using the commercial CFD package CFX4.2.

Particle trajectories are presented for different particle sizes and velocity combinations, including investigations of the influence of the swirl, which is set up at the inlet to the probe by the use of swirl vanes. The results suggest that the modified probe is capable of separating particles down to sizes of 5 μm. None of the 16 combinations of velocities in the inner and middle tube are predicted to cause any particle to be sucked into the middle tube.

Testing and optimisation of probe. The probe then was tested in a model-scale spray dryer with an atomiser giving a lower particle size distribution than that in a full-scale dryer. Experiments with droplets showed that they could be separated down to 5 μm with no visible contamination of the thermocouple or the middle tube, given a sufficient air velocity in the outer tube.

However, further tests with wet solid particles led to decreased separation efficiency due to clogging of the swirl vanes. This left the device using only one separation mechanism, namely the flow reversal.

It was found that the optimal flow rates varied according to whether measurements were being taken in the liquid or powder region of the dryer, due to the fact that powder clogs up the swirl vanes and prevents swirl formation.

It is recommended that a middle tube velocity of 2 m/s and an outer tube velocity of 12 m/s should be used while taking measurements in both droplet and particle-laden flows.

Both the results of the numerical simulations and of the tests in a model scale dryer indicate that the modified probe will work well and will prove to be a powerful device to measure the temperature and humidity patterns in liquid sprays.

8. Conclusions

Both simulations and experiments have shown that the improved sampling probe is a valuable tool for gas temperature and humidity measurements in two-phase flow. The best performance has been determined theoretically and experimentally at high inlet velocities and low inner velocities. It is recommended that a middle tube velocity of 2 m/s and an outer tube velocity of 12 m/s should be used while taking measurements in both droplet and particle-laden flows.

Acknowledgements

The authors wish to thank the Australian Dairy Research and Development Corporation for financial support under the project number US087.

References

[1] Anonymous: CFX-4.2 Solver, User Manual, AEA Technology, Harwell Laboratory, Didcot, Oxfordshire, UK, 1997.
[2] D.F. Fletcher, B.S. Haynes, A.A. Sola, S.D. Joseph, Mathematical modelling of a rotary swirl cyclone scrubber, Chem. Eng. Commun. 101 (1997) 65–87.
[3] V. Gnielinski, New equations for heat and mass transfer in turbulent pipe and channel flow, Int. J. Chem. Eng. 16 (1976) 359–368.
[4] J. Goldberg, Modelling of spray dryer performance, Ph.D. Thesis, University of Oxford, UK, 1987.
[5] A.K. Gupta, D.G. Lilley, N. Syred, Swirl Flows, Abacus Press, Turnbridge Wells, UK, 1984.
[6] F.G. Kieviet, J. Van Raaij, P.J.A.M. Kerkhof, A device for measuring temperature and humidity in a spray drying chamber, Trans. Inst. Chem. Engrs 75 (1997) 329–333.
[7] F.G. Kieviet, P.J.A.M. Kerkhof, Air flow, temperature and humidity patterns in a co-current spray dryer: modelling and measurements, Drying Technol. 15(6-8) (1997) 1763–1773.
[8] B.E. Launder, D.B. Spalding, The numerical computation of turbulent flows, Comput. Methods Appl. Mech. Eng. 3 (1974) 269–289.
[9] S. Nijhawan, J.C. Chen, R.K. Sundaram, E.J. London, Measurements of vapor superheat in post-critical-heat-flux boiling, J. Heat Transfer 102 (1980) 465–470.

[10] S.E. Papadakis, Air temperatures and humidities in spray drying, Ph.D. Thesis, University of California, Berkeley, CA, 1987.
[11] C.M. Rhie, W.L. Chow, Numerical study of the turbulent flow past an airfoil with trailing separation, AIAA J. 21 (1983) 1527–1532.
[12] N.A. Shore, B.S. Haynes, D.F. Fletcher, Numerical aspects of swirl, Computational Techniques and Applications: CTAC95, Swinburne University of Technology, Melbourne, Australia, 1995, pp. 693–700.
[13] J.S. Shuen, L.D. Chen, G.M. Faeth, Evaluation of a stochastic model of particle dispersion in a turbulent round jet, Am. Inst. Chem. Engrs J. 29 (1983) 167.